Self-Consistent Energy Bands of Metallic Copper by the Augmented-Plane-Wave Method*

E. C. SNOW AND J. T. WABER
University of California, Los Alamos Scientific Laboratory, Los Alamos, New Mexico

The band structure, Fermi surface, and density of states from a self-consistent augmented-plane-wave (APW) calculation of copper are presented and compared with previously reported results. Some results of a self-consistent APW calculation in which the exchange term was reduced to $\frac{2}{3}$ of the original Slater term are also reported.

INTRODUCTION

APPARENTLY, the first attempt to perform a self-consistent band calculation was made in 1936 by Ewing and Seitz,[1] for both LiH and LiF. They used the wave functions for the point Γ in the Brillouin zone to generate each new potential. No exchange terms were included. In 1942, Manning[2] used a similar Wigner-Seitz or cellular method for bcc iron. He obtained the wave functions for six different energies lying in the d bands and used these in generating his next potential, but made no correction for exchange. Wakoh[3] used a slightly different procedure for copper and nickel in 1965. For the sp band, he found the wave function corresponding to the energy $E(\Gamma)+0.6E_f$, where $E(\Gamma)$ is the energy for $k=0$ and E_f is the Fermi energy. For the d bands, he obtained the wave functions corresponding to five equally spaced energies, and the resulting charge densities were weighted to generate the next potential. He employed Slater's $\rho^{1/3}$ method[4] for correcting the exchange in both the atom and the metal.

Other SCF cellular calculations have been made, using conventional atomic methods while imposing appropriate boundary conditions of the surface of the Wigner-Seitz sphere. For example, Ridley[5] approximated the band structure of the bcc phase of uranium in 1958 using Hartree wave functions. Waber, Liberman, and Cromer[6] used the relativistic Dirac-Slater wave functions with exchange in 1965 for fcc cerium.

Herman[7] has described his empirically perturbed self-consistent method in which he obtains the self-consistent wave functions at 32 points in the Brillouin zone. A perturbing potential is then added to gain better agreement with optical data, that is, to bring "··key features of the theoretical energy-level spectrum into agreement with the most reliably established features of the experimental spectrum."

The first full-fledged, self-consistent band calculation was made by Switendick[8] for nonmagnetic chromium in 1965. Another important self-consistent calculation was made by De Cicco[9] in 1965 for KCl. The latter two authors have employed APW calculations coupled with Slater's form of exchange. The wave functions were obtained for 256 points in the Brillouin zone, spherically averaged, and summed over the occupied states before being used to generate the new crystal potential.

In 1954, Gasper[10] and in 1966, Tong and Sham[11] have questioned the magnitude of the Slater exchange approximation. In their derivations, they obtained an exchange approximation which was $\frac{2}{3}$ as large as Slater proposed. Slater,[12] after reviewing their arguments, still favored the original exchange potential for atomic self-consistent-field (SCF) calculations. In 1966, Cowan *et al.*[13] showed that better agreement with Hartree-Fock calculations was obtained when $\frac{2}{3}$ of the Slater exchange term was used in both relativistic Dirac-Slater and nonrelativistic Hartree-Fock-Slater atomic calculations. Tong and Sham[11] reached a similar conclusion in their nonrelativistic study. Slater[12] also discussed reasons why the self-consistent Hartree-Fock atomic orbitals might not be the best starting point for solid-state calculations.

In the work reported here, a self-consistent APW method was used to determine the band structure, Fermi surface, and density of states for metallic copper from a sampling at the 2048 points in the Brillouin zone of the type $(\pi/2a)(n/8,m/8,p/8)$. To determine whether better agreement with experiment could be achieved in band calculations by using the original statistical exchange potential or its reduced value, self-consistent APW calculations were made for copper in which the coefficient of the Slater exchange term was both $\frac{2}{3}$ and 1. Some of the results of these calculations are reported below.

The present study of the self-consistent bands was conducted on copper for several reasons. Copper is one

* Work performed under the auspices of the U. S. Atomic Energy Commission.

[1] D. H. Ewing and F. Seitz, Phys. Rev. **50**, 760 (1936).
[2] M. F. Manning, Phys. Rev. **63**, 190 (1943).
[3] Shinya Wakoh, J. Phys. Soc. Japan **20**, 1894 (1965).
[4] J. C. Slater, Phys. Rev. **81**, 385 (1951).
[5] E. C. Ridley, Proc. Roy. Soc. (London) **A247**, 199 (1958).
[6] J. T. Waber, D. Liberman, and D. T. Cromer, *Rare Earth Research III* (Gordon and Breach Science Publishers, Inc., New York, 1965), pp. 187–202.
[7] F. Herman, R. L. Kortum, C. D. Kuglin, and R. A. Short, in *Quantum Theory of Atoms, Molecules, and the Solid State*, edited by P. O. Löwdin (Academic Press Inc., New York, 1966).
[8] A. C. Switendick, J. Appl. Phys. **37**, 1022 (1966).
[9] P. De Cicco, MIT Solid State and Molecular Theory Group, Quarterly Progress Report, No. 56 (1965).
[10] R. Gasper, Acta Phys. Hung. **3**, 263 (1954).
[11] B. Y. Tong and L. J. Sham, Phys. Rev. **144**, 1 (1966).
[12] J. C. Slater, MIT Solid State and Molecular Theory Group, Quart. Progr. Report, No. 58, 1965 (unpublished).
[13] R. D. Cowan, A. C. Larson, D. Liberman, J. B. Mann, and J. Waber, Phys. Rev. **144**, 5 (1966).

of the more difficult elements to converge to self-consistency in atomic SCF calculations. Previous band calculations by Burdick[14] and Mattheiss[15] using the APW method and Segall[16] using the Green's-function method had been done on it. In addition, there is an extensive amount of experimental information available for copper. Probably only aluminum has a comparable background, and its atomic SCF calculation converges rapidly.

THEORY

1. Self-Consistent APW Method

A self-consistent APW calculation, as any such self-consistent calculation, begins with a starting potential, the determination of which will be discussed later. This potential was used in determining the eigenvalues associated with each of 256 equally spaced points in the Brillouin zone for the face-centered cubic lattice. A detailed description of the method of locating these eigenvalues with the APW program is given by Burdick.[14] Because of the symmetry of the Brillouin zone, calculations for the points within 1/48 of the zone are sufficient to determine the eigenvalues for all the points in the zone. For the 256 points of the type $(n/4, m/4, p/4)$ in the Brillouin zone about 20 such calculations are required.

To determine the Fermi level, each of the eigenvalues, which represents a state in momentum space, is assigned a weight $[W(\mathbf{k})]$ given by

$$W(\mathbf{k})=2\times\frac{d_{\mathbf{k}}\cdot n_{\mathbf{k}}}{N}, \tag{1}$$

where d_k is the degeneracy of the eigenvalue, n_k is the number of points in the star of $\mathbf{k}$, and N is the total number of equally spaced points in the Brillouin zone, in this case 256. These states were filled, in the order of increasing energy, until the sum of the weights (of the filled states) equals the number of electrons contained in the bands. The energy of the highest filled state (at 0°K), is considered to be the Fermi energy. In practice, because $E(\mathbf{k})$ is obtained for a small number of points, the sum of these weights never exactly equals the number of electrons, and the Fermi energy is determined by interpolating between the energies of the highest filled and the next unfilled state.

With the Fermi level located, the next step is to determine the resulting radial charge density of the occupied band states. It should be noted that since the configuration and charge density of the core electrons are considered to be unchanged, it is unnecessary to consider any calculations for states below the valence bands. To determine the radial charge density of the bands, the wave function associated with each eigenvalue must be obtained. These wave functions are linear combinations of augmented plane waves. As described by Slater,[17]

$$\psi=\sum_i C_i\psi_i, \tag{2}$$

where the C_i's are the coefficients of the augmented plane waves and depend upon $\mathbf{k}$. The spherical average of the wave function and its radial charge density were determined for each calculated state $E(\mathbf{k})$. Then the individual charge densities were normalized to unity. To get the total radial charge density, the radial charge densities for all the states below the Fermi level were summed according to the relation

$$\rho(r)=\sum_{E(\mathbf{k})}^{Ef} W(\mathbf{k})\cdot\rho(r,E(\mathbf{k})), \tag{3}$$

where $W(\mathbf{k})$ is the weight of a state at the point $\mathbf{k}$, and $\rho(r,E(\mathbf{k}))$ is the spherically symmetrical radial change density associated with the eigenvalue $E(\mathbf{k})$. A more detailed description of this process is given by Ern and Switendick.[18] The total charge density inside the APW sphere, a sphere inscribed in the Wigner-Seitz cell, is then determined by summing the charge densities of the bands and core states. The charge density in the "annular" volume between the APW sphere and the cell boundary is considered to be uniformly distributed and represents enough charge to make the net charge of the cell zero .

The potential for the next iteration is determined from a charge density that is a mixture of the input charge density from which the starting potential was generated and the resulting output charge density described above. The details of the determination of this new potential are given below.

This process was repeated through several iterations, until the calculation was considered self-consistent.

Once self-consistency was achieved, the calculation was extended to cover 2048 points in the Brillouin zone. In addition, a 2048-point calculation was undertaken before self-consistency was reached to determine whether the larger calculation should be used. It was found that the total charge densities resulting from the 256-point and 2048-point calculations differed by about 2%. At the same time, the total charge density from two successive iterations using 256 points differed by about 10%. Thus, the variation between the 256-point and 2048-point calculations is about $\frac{1}{5}$ of the variation between successive iterations. It was decided that use of the larger calculation at an early stage of convergence would be a waste of machine time. However, once self-consistency had been achieved, the effect of the larger calculation on the Fermi level and surface was significant. The Fermi level resulting from

[14] G. A. Burdick, Phys. Rev. **129**, 138 (1963).
[15] L. F. Mattheiss, Phys. Rev. **134**, A970 (1964).
[16] B. Segall, Phys. Rev. **125**, 109 (1962).
[17] J. C. Slater, Phys. Rev. **51**, 846 (1937).
[18] V. Ern and A. C. Switendick, Phys. Rev. **137**, A1927 (1965).

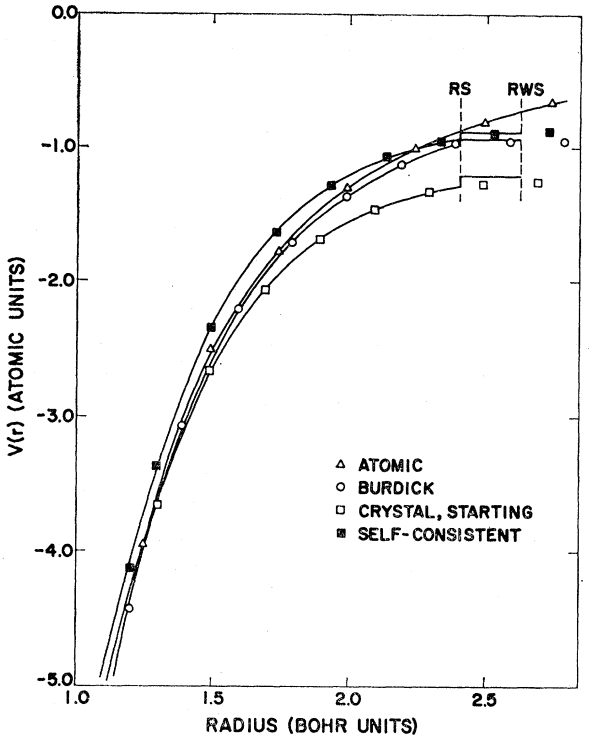

FIG. 1. Comparison of the initial and self-consistent potentials with the atomic potential and with the Chodorow potential used by Burdick (Ref. 14).

the 2048-point calculation was about 5% more positive than that obtained with the 256-point calculation. The use of more points results in an increase of the neck diameter by a factor of 3 and a significant change in the belly diameter. It was, therefore, desirable to extend the calculation to 2048 points, after self-consistency has been achieved for the smaller number of points, and then to proceed to a new set of self-consistent bands.

The self-consistency criteria used in all these calculations were that $|\Delta E(\mathbf{k})|$ for every point in the zone be less than 0.002 Ry between successive iterations. It is interesting to note that when these criteria were met, the difference between the radial charge density of successive iterations was less than 1% everywhere in the radial range.

2. The Potentials

The potential used in the APW calculations is a muffin-tin type. That is, it is spherically symmetric inside the APW spheres and is constant everywhere else in the cell. In the present work, the radius of the APW sphere (R_S) was chosen to be one-half the nearest-neighbor distance in the face-centered cubic lattice. This means that the APW spheres are inscribed in the Wigner-Seitz cells, as mentioned earlier. The Wigner-Seitz sphere, which is also used in the calculation, is that sphere which has the same volume as the Wigner-Seitz cell; it has a radius (R_{WS}) given by

$$R_{WS}=(3/4\pi)^{1/3}a_0,$$

where a_0 is the lattice constant of the fcc lattice.

The procedure described by Mattheiss[19] was used to generate the starting potential of the self-consistent APW calculations from a superposition of the atomic potentials of the first four nearest neighbors in the fcc lattice. This procedure, through use of Löwdin's α-function expansion method,[20] involves an expansion of the spherically symmetric potentials of the nearest neighbors.

The exchange was determined by Slater's free-electron approximation, as mentioned earlier. The constant potential selected was the average of the potential in the annular volume between the APW sphere and the Wigner-Seitz sphere. The atomic potentials used in generating the starting potentials for these calculations were obtained from the atomic self-consistent Dirac-Slater calculation by Liberman, Waber, and Cromer.[21] A plot of the starting crystal potential used in this self-consistent APW calculation is given in Fig. 1.

The potentials for the second and following iterations were determined from a mixture of input and output charge densities, the solution to the Poisson equation being given by

$$V(r)=\frac{2Z}{r}-\frac{2}{r}\int_0^r\rho(r')dr'+2\int_r^\infty\frac{\rho(r')}{r'}dr',$$

where Z is the atomic number, r is the radius, and $\rho(r')$ is the radial charge density. The Slater free-electron approximation was used to determine the exchange term. The value of the constant potential was

$$V_c=V(R_S)+V_{ex}(\text{Out})-V_d,$$

where $V(R_S)$ is the Coulomb potential at the APW sphere radius, $V_{ex}(\text{Out})$ is the value of the constant exchange potential between spheres, and V_d is the Coulomb discontinuity at the APW sphere boundary. In order to determine the value of $V_{ex}(\text{Out})$ and V_d (quantities which are discussed below), the charge between spheres was considered to be uniformly distributed. The resulting constant charge density is then given by

$$\rho_c=\frac{Z-\int_0^{RS}\rho(r)dr}{\Omega_{WS}-\Omega_S},$$

where Ω_{WS} is the volume of the Wigner-Seitz cell and Ω_S is the volume of the APW sphere. The resulting constant charge density was then used to determine the Slater exchange outside the APW sphere. Use of this

[19] L. F. Mattheiss, Phys. Rev. 133, A1399 (1964).
[20] P. O. Löwdin, Advan. Phys. 5, 1 (1956).
[21] D. Liberman, J. T. Waber, and D. T. Cromer, Phys. Rev. 137, A27 (1965).

value for the constant exchange potential automatically includes the exchange discontinuity at the APW sphere boundary in the value of the constant potential V_c.

To determine the Coulomb discontinuity V_d at the sphere boundary, the Ewald method[22] of solving the Madelung problem was used. The adaptation of this method to the APW problem is described in detail by Slater and De Cicco.[23] In their presentation, they show that the Coulomb discontinuity at the APW sphere boundary is given by

$$V_d = 0.107123(Q/a_0),$$

where a_0 is the lattice constant of the fcc lattice, and Q is the net uniform negative "sea" of charge surrounding the nuclear "point" charge of equal magnitude and opposite sign. The value of Q used in this problem was derived by extending the constant charge density between spheres inward to the nucleus at $r=0$, and is given by

$$Q=\rho_c\Omega_{WS},$$

where, as before, ρ_c is the constant charge density and Ω_{WS} is the volume of the Wigner-Seitz cell.

TABLE I. Potential of self-consistent copper for $0<r<2.5$ [r in Bohr units and $V(R)$ in atomic units].

0.005	11393.812	0.360	59.703	1.200	4.136
0.010	5591.365	0.380	54.158	1.220	3.966
0.015	3657.495	0.400	49.298	1.240	3.806
0.020	2691.454	0.420	45.013	1.260	3.654
0.025	2113.093	0.440	41.211	1.280	3.510
0.030	1728.531	0.460	37.822	1.300	3.375
0.035	1454.762	0.480	34.786	1.320	3.246
0.040	1250.188	0.500	32.057	1.340	3.124
0.045	1091.716	0.520	29.596	1.360	3.008
0.050	965.495	0.540	27.370	1.380	2.899
0.055	862.707	0.560	25.353	1.400	2.795
0.060	777.489	0.580	23.521	1.420	2.696
0.065	705.774	0.600	21.854	1.440	2.602
0.070	644.667	0.620	20.334	1.460	2.513
0.075	592.033	0.640	18.947	1.480	2.428
0.080	546.276	0.660	17.678	1.500[a]	2.347
0.085	506.166	0.680	16.517	1.540	2.197
0.090	470.749	0.700	15.453	1.580	2.061
0.095	439.266	0.720	14.476	1.620	1.938
0.100[a]	411.115	0.740	13.578	1.660	1.827
0.110	362.941	0.760	12.751	1.700	1.725
0.120	323.289	0.780	11.990	1.740	1.633
0.130	290.138	0.800	11.287	1.780	1.550
0.140	262.062	0.820	10.637	1.820	1.474
0.150	238.022	0.840	10.037	1.860	1.405
0.160	217.240	0.860	9.480	1.900	1.342
0.170	199.128	0.880	8.964	1.940	1.285
0.180	183.227	0.900	8.485	1.980	1.234
0.190	169.174	0.920	8.040	2.020	1.188
0.200	156.682	0.940	7.625	2.060	1.146
0.210	145.517	0.960	7.239	2.100	1.108
0.220	135.490	0.980	6.878	2.140	1.074
0.230	126.445	1.000	6.542	2.180	1.043
0.240	118.252	1.020	6.227	2.220	1.016
0.250	110.804	1.040	5.932	2.260	0.992
0.260	104.011	1.060	5.656	2.300	0.970
0.270	97.797	1.080	5.397	2.340	0.952
0.280	92.097	1.100	5.153	2.380	0.935
0.290	86.857	1.120	4.925	2.420[b]	0.922
0.300[a]	82.028	1.140	4.710	2.460	0.910
0.320	73.444	1.160	4.507	2.500	0.900
0.340	66.075	1.180	4.316		

[a] Points where the mesh size is doubled.
[b] Radius of APW sphere.

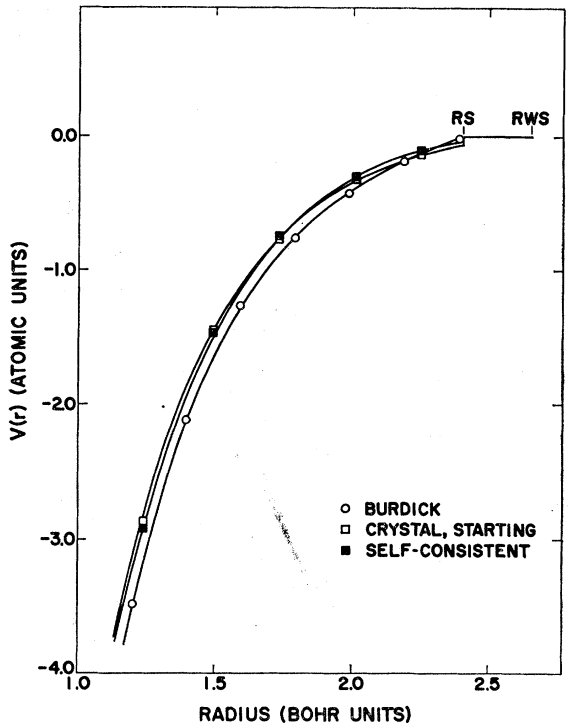

FIG. 2. Comparison of the initial and self-consistent potentials with the Chodorow potential, all shifted so that $V_c=0.0$ Ry.

A plot of the final self-consistent potential of this calculation is given in Fig. 1. Figure 2 shows a comparison of the self-consistent potential, the starting potential, and the Chodorow potential used by Burdick,[14] as the APW program would "see" them, that is, they are shifted so that $V_c=0$. The values of the final self-consistent potential resulting from this calculation are listed in Table I for $0<r<2.5$ Bohr units. The value of the constant potential for the self-consistent case was -0.88278 Ry.

In using the above method of determining the potentials, it was recognized that a constant of integration had not been determined. The effect is that the constant potential is in error by a small shift, which must be determined to properly locate the bands and Fermi energy. This shift used was the energy necessary to make the $1s$ eigenvalue of the $1s$ electrons in the self-consistent potential coincide with the $1s$ eigenvalue of the starting potential. Since the value of the constant of the starting potential was completely determined, it is felt that the location of the $1s$ eigenvalue is known at this point. It is also felt that since the charge density inside the $1s$ radius is virtually unchanged, leaving the $1s$ wave function also unchanged, and that the redistribution of the

[22] P. P. Ewald, Ann. Physik **64**, 253 (1921).
[23] J. C. Slater and P. De Cicco, MIT Solid State and Molecular Theory Group, Quarterly Progress Report, No. 50, 1963 (unpublished).

TABLE II. Eigenvalues of points in 1/48 of the Brillouin zone considering 2048 points in the entire zone, given with respect to $V_c=0$.

	K	Band 1		Band 2		Band 3		Band 4		Band 5		Band 6	
Γ	(000)/4	1	0.01771	25′	0.23530	25′	0.23530	25′	0.23530	12	0.28208	12	0.28208
X	(080)/4	1	0.13574	3	0.15805	2	0.31604	5	0.32824	5	0.32824	4′	0.73495
L	(444)/4	1	0.15195	3	0.23275	3	0.23275	3	0.31892	3	0.31892	2′	0.53548
K&U	(660)/4	1	0.16636	1	0.18537	3	0.26684	4	0.29240	2	0.31638	3	0.91044
Δ	(010)/4	1	0.03264	2′	0.23267	5	0.23870	5	0.23870	1	0.28077	2	0.28491
Δ	(020)/4	1	0.06634	2′	0.22381	5	0.24731	5	0.24731	1	0.27418	2	0.28862
Δ	(030)/4	1	0.11792	2′	0.21075	5	0.26111	5	0.26111	1	0.27217	2	0.29441
Δ	(040)/4	1	0.15664	2′	0.19556	5	0.27771	5	0.27771	2	0.30097	1	0.30558
Δ	(050)/4	1	0.15981	2′	0.18063	5	0.29591	5	0.29591	2	0.30761	1	0.39767
Δ	(060)/4	1	0.14946	2′	0.16821	5	0.31196	5	0.31196	2	0.31330	1	0.52480
Δ	(070)/4	1	0.14011	2′	0.15948	2	0.31713	5	0.32389	5	0.32389	1	0.65978
Z	(180)/4	1	0.14049	4	0.16071	1	0.31361	3	0.31637	2	0.32826	3	...
Z	(280)/4	1	0.15322	4	0.17204	3	0.28584	1	0.30340	2	0.32830	3	...
Z	(380)/4	1	0.16840	4	0.19115	3	0.25031	1	0.29084	2	0.32837	3	...
W	(480)/4	2′	0.17534	3	0.21750	3	0.21750	1	0.28418	1′	0.32867		...
Λ	(111)/4	1	0.05458	1	0.23128	3	0.24211	3	0.24211	3	0.28241	3	0.28241
Λ	(222)/4	1	0.13706	3	0.24543	3	0.24543	1	0.24804	3	0.29011	3	0.29011
Λ	(333)/4	1	0.15543	3	0.23815	3	0.23815	3	0.31012	3	0.31012	1	0.39437
Q	(471)/4	−	0.18490	+	0.20806	−	0.22544	+	0.28146	+	0.32127	−	...
Q	(462)/4	+	0.18566	−	0.20635	−	0.24993	+	0.26275	+	0.31663	−	0.72154
Q	(453)/4	+	0.16222	−	0.22558	+	0.24120	−	0.29117	+	0.31796	−	0.59282
Σ	(110)/4	1	0.04259	3	0.23136	2	0.23983	1	0.24109	4	0.27959	1	0.28472
Σ	(220)/4	1	0.11020	3	0.22154	1	0.24857	2	0.25121	4	0.27104	1	0.29906
Σ	(330)/4	1	0.18428	3	0.21415	1	0.24223	4	0.26398	2	0.26773	1	0.36599
Σ	(440)/4	1	0.20906	3	0.21544	1	0.22849	4	0.26456	2	0.28535	1	0.52118
Σ	(550)/4	1	0.19082	1	0.21156	3	0.23290	4	0.27486	2	0.30256	−	...
S	(181)/4	1	0.14498	1	0.16383	3	0.30784	4	0.30813	2	0.32522	−	...
	(120)/4	+	0.07786	−	0.22401	−	0.24743	+	0.24765	+	0.27481	+	0.28951
	(130)/4	+	0.12769	−	0.21195	+	0.25152	−	0.26101	+	0.27948	+	0.29881
	(140)/4	+	0.16421	−	0.19758	+	0.25984	−	0.27758	+	0.29798	+	0.33052
	(150)/4	+	0.16589	−	0.18343	+	0.27773	−	0.29578	+	0.30823	+	0.41982
	(160)/4	+	0.15460	−	0.17096	+	0.29448	−	0.31218	+	0.31354	+	0.54603
	(170)/4	+	0.14489	−	0.16311	+	0.30732	+	0.31655	−	0.32422	+	0.68250
	(230)/4	+	0.15373	−	0.21415	+	0.24522	−	0.26245	+	0.27308	+	0.32297
	(240)/4	+	0.18370	−	0.20240	+	0.23937	−	0.27741	+	0.28643	+	0.37530
	(250)/4	+	0.18204	−	0.19140	+	0.24989	−	0.29521	+	0.29851	+	0.47131
	(260)/4	+	0.16869	−	0.18123	+	0.26546	+	0.30447	−	0.31207	+	0.60009
	(270)/4	+	0.15791	−	0.17442	+	0.27926	+	0.30496	−	0.32435	+	...
	(340)/4	+	0.20444	−	0.20996	+	0.22888	+	0.27209	−	0.27945	+	0.43691
	(350)/4	+	0.20246	−	0.20356	+	0.22528	+	0.28432	−	0.29542	+	0.54181
	(360)/4	+	0.18578	−	0.19724	+	0.23581	+	0.29059	−	0.31175	+	0.67519
	(370)/4	+	0.17348	−	0.19276	+	0.24591	+	0.29150	−	0.32409	+	...
	(450)/4	+	0.20541	+	0.21656	−	0.21858	+	0.27280	−	0.29752	+	0.63177
	(460)/4	+	0.19232	+	0.21351	−	0.21857	+	0.28052	−	0.31187	+	...
	(470)/4	+	0.18016	+	0.21610	−	0.21787	+	0.28365	−	0.32394	+	...
	(560)/4	+	0.18058	+	0.19993	−	0.24354	+	0.28341	−	0.31322	+	...
B	(570)/4	+	0.17182	+	0.19284	−	0.24884	+	0.28886	−	0.32398	+	...
	(121)/4	+	0.08866	+	0.22594	+	0.24715	−	0.24746	+	0.27829	−	0.28860
	(131)/4	+	0.13559	+	0.21536	+	0.24931	−	0.25600	+	0.29072	−	0.29708
	(141)/4	+	0.16817	+	0.20162	+	0.25394	−	0.26847	−	0.30607	+	0.34094
	(151)/4	+	0.16943	+	0.18735	+	0.27191	−	0.28236	−	0.31483	+	0.43654
	(161)/4	+	0.15895	+	0.17473	+	0.29030	−	0.29609	−	0.32148	+	0.56455
	(171)/4	+	0.14939	+	0.16655	+	0.30319	−	0.30633	−	0.32454	+	...
	(221)/4	+	0.11813	+	0.22856	+	0.24782	−	0.24849	−	0.27816	+	0.29627
	(231)/4		0.15151		0.22452		0.24404		0.25092		0.27375		0.31927
	(241)/4		0.17620		0.21676		0.24038		0.26371		0.30215		0.37906
	(251)/4		0.17771		0.19987		0.25023		0.27691		0.31334		0.48137
	(261)/4		0.16995		0.18555		0.26429		0.28982		0.31992		0.61337
	(271)/4		0.16105		0.17770		0.27641		0.29824		0.32328		...
	(281)/4	+	0.15683	+	0.17523	−	0.28160	+	0.30057	−	0.32445	+	...
	(331)/4	+	0.17213	+	0.23376	+	0.24612	−	0.25196	−	0.28205	+	0.36376
	(341)/4		0.18298		0.22994		0.23768		0.26037		0.29387		0.43888
	(351)/4		0.18744		0.21304		0.23552		0.27144		0.30703		0.54715
	(361)/4		0.18470		0.19880		0.23979		0.28168		0.31595		0.68236
	(371)/4		0.17625		0.19396		0.24591		0.28746		0.32174		...
	(381)/4	+	0.17182	+	0.19284	−	0.24884	+	0.28886	−	0.32398	+	...
	(441)/4	+	0.18771	+	0.22282	+	0.24828	−	0.25637	−	0.29435	+	0.52270
	(451)/4		0.19275		0.21171		0.24086		0.26495		0.30458		0.63242
	(461)/4		0.19948		0.19993		0.23307		0.27468		0.31430		...
	(551)/4	+	0.18870	+	0.20868	+	0.24317	−	0.26780	−	0.30856		...
	(561)/4		0.18249		0.20007		0.24511		0.27790		0.31591		...
	(232)/4	+	0.15632	+	0.24174	−	0.24607	+	0.25755	−	0.30257	+	0.31739
	(242)/4	+	0.16904	+	0.23214	+	0.25073	−	0.25219	−	0.31339	+	0.39887

TABLE II (*continued*)

	K	Band 1	Band 2	Band 3	Band 4	Band 5	Band 6
	(252)/2	+ 0.17451	+ 0.21314	+ 0.25172	− 0.26164	− 0.31985	+ 0.51198
	(262)/4	+ 0.17400	+ 0.19688	+ 0.25797	− 0.27406	− 0.32197	+ 0.64914
	(272)/4	+ 0.16983	+ 0.18807	+ 0.26429	− 0.28627	− 0.31966	+ ...
	(332)/4	+ 0.16025	+ 0.23886	− 0.24209	+ 0.28444	− 0.29664	+ 0.36200
	(342)/4	0.16636	0.23161	0.24531	0.27351	0.30959	0.44832
	(352)/4	0.17399	0.21931	0.25196	0.26173	0.31751	0.56232
	(362)/4	0.18092	0.20617	0.24946	0.26695	0.31901	...
	(372)/4	0.18249	0.20007	0.24511	0.27790	0.31591	...
	(442)/4	+ 0.16837	+ 0.22744	− 0.24460	+ 0.28117	− 0.30697	+ 0.52704
	(452)/4	0.17493	0.21821	0.25112	0.26736	0.31398	0.62640
F	(552)/4	+ 0.17978	+ 0.21544	− 0.25664	+ 0.26349	− 0.31294	+ 0.68359
	(343)/4	+ 0.15740	+ 0.23211	− 0.23843	+ 0.29916	− 0.31735	+ 0.47767
	(353)/4	+ 0.16524	+ 0.22408	− 0.24477	+ 0.28070	− 0.32004	+ 0.58231
	(363)/4	+ 0.17718	+ 0.21389	− 0.25540	+ 0.26088	− 0.31639	+ 0.68242
F	(443)/4	+ 0.15613	+ 0.23149	− 0.23598	+ 0.30794	− 0.31596	+ 0.53256

charge density outside this radius should have very little effect on the outer shielding of the $1s$ electron, the $1s$ eigenvalue of the self-consistent calculation should be insignificantly different from the $1s$ eigenvalue of the starting potential. The resulting shift for this self-consistent calculation was found to be −0.09264 Ry. Adding this shift, the correct value for the constant potential becomes −0.97542 Ry. It is interesting to note that the $1s$ eigenvalue of the crystal starting potential was somewhat more negative in energy than the $1s$ of the free atom.

RESULTS

1. Energy-Band Structure

All the results presented in this paper came from self-consistent calculations which covered 2048 equally spaced points in the Brillouin zone. The resulting eigenvalues for all the points in 1/48 of the zone are listed in Table II. It should be noted that these eigenvalues are given with respect to a constant potential of zero between spheres. To locate these eigenvalues correctly, one needs to add the proper constant potential value to them, in this case −0.97542 Ry.

Figure 3 shows the resulting self-consistent $E(\mathbf{k})$ curves in the direction of high symmetry. The dashed line below the $E(\mathbf{k})$ curves represents the value of the constant potential V_c. The dot-dash line, denoted by E_f, represents the location of the Fermi energy. All energies represented by these curves, have been located with respect to $V_c = -0.97542$ Ry between spheres. Figure 4 is a comparison of the bands in the Γ-X direction for the initial iteration and for the final self-consistent result. The most significant difference between these two sets of curves is the width of the d band and the relative position of the d band with respect to the sp band. The sp band is considered to lie in the range of energies from Γ_1 to $X_{4'}$, indicated on the figure by the dashed transition curves connecting the two portions of the Δ_1 curves. The d band is considered to lie in the range of energies from X_1 to X_5. With this in mind, it can be seen that, as the calculation goes to self-consistency, the d band becomes narrower and more negative in energy with respect to the sp band. It may also be noted that all the bands shift to slightly higher energies as self-consistency is achieved. Table III gives the energy differences of states which indicate the relative positions and widths of the sp and d bands. The energy differences of $\Gamma_{25'}-\Gamma_1$ and and $X_5-\Gamma_1$ indicate the location of the top of the d band with respect to the bottom of the sp band. The energy difference of X_5-X_1 gives the width of the d band, while that of $X_{4'}-\Gamma_1$ gives the width of the sp band. The energy difference of E_f-X_5 indicates the location of the top of the d band with respect to the Fermi energy. The results of two self-consistent calculations are given in this table. The "Slater=1" is the calculation in which the original Slater exchange approximation was used, while the "Slater=$\frac{2}{3}$" is the calculation in which this exchange term was reduced to $\frac{2}{3}$ of its original value.

2. Fermi Energy and Surface

The Fermi energy for the self-consistent calculation, determined from the eigenvalues for 2048 points in the

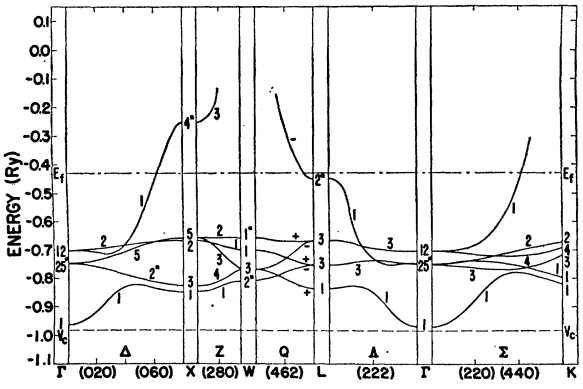

FIG. 3. $E(\mathbf{k})$ curves for self-consistent copper in directions of high symmetry.

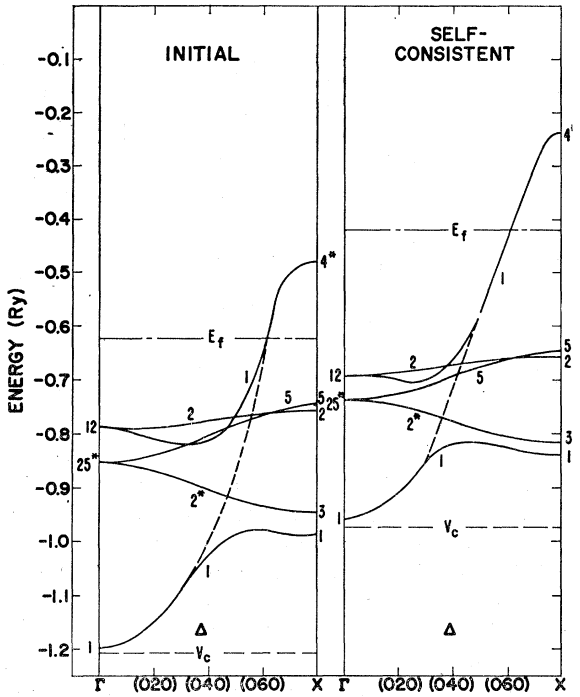

FIG. 4. Comparison of $E(\mathbf{k})$ curves in the Γ to X direction for the initial and self-consistent calculations.

Brillouin zone, was found to be −0.41947 Ry or −5.71 eV. Intersections of the (100) and (110) planes with the Fermi surface for the self-consistent calculations are given in Fig. 5. In this figure, the area Γ, K, L, U, X, and Γ is in the (110) plane and the area Γ, K, W, X, and Γ is in the (100) plane. The "neck" and "belly" radii of the Fermi surface of copper for the present calculation, previous calculations, and experimental results are given in Table IV. It should be noted that use of the reduced exchange results in a significant increase in the "neck" radius and in an increased difference between "belly" radii in ⟨100⟩ and ⟨110⟩ directions, i.e., in an increased asphericity of the Fermi surface.

TABLE III. Energy differences for states which indicate position and width of the sp and d bands (in rydbergs).

	$\Gamma_{25'}-\Gamma_1$	$X_5-\Gamma_1$	X_5-X_1	$X_{4'}-\Gamma_1$	E_f-X_5
Segall[a]	0.331	0.470	0.300	0.807	0.183
Burdick[b]	0.399	0.512	0.249	0.804	0.143
Mattheiss[c]	0.463	0.570	0.252	0.794	···
Wakoh[d]	0.386	0.499	0.245	···	0.159
Spicer[e]	···	···	0.205[g]	···	0.147[g]
Lettington[f]	···	···	···	···	0.147[g]
Present:					
Slater=1	0.216	0.308	0.191	0.717	0.228
Slater=⅔	0.392	0.508	0.262	0.720	0.111

[a] Reference 16.
[b] Reference 14.
[c] Reference 15.
[d] Reference 3.
[e] C. N. Berglund and W. E. Spicer, Phys. Rev. **136**, A1044 (1964).
[f] A. H. Lettington, Phys. Letters **9**, 98 (1964).
[g] Obtained from photoemission studies.

3. Density of States

A density of states histogram resulting from the self-consistent solution for 2048 points is given in Fig. 6. In this histogram, the energies are given with respect to zero energy between spheres. The starting point is at $E=0$ Ry and the bar width $\Delta E=0.025$ Ry. In making the histograms for the self-consistent calculation, it was found that the fine structure depends strongly on the energy at which the first bar is started. To stabilize the fine structure, several histograms with the same ΔE but different starting energies were averaged. The starting values used were determined by

$$E_n=E_0-\frac{\Delta E(n-1)}{N}, \quad n=1,2,3,\cdots,N,$$

where E_0 was chosen to be the lowest energy for which states exist in the conduction bands, ΔE is the histogram bar width, and N is the number of histograms to be averaged. It was found that for $\Delta E=0.025$ Ry, N need not be larger than 5. The resulting averaged histogram has a bar width of $\Delta E/N$ and a bar height which is the average height of the bars in the N histograms that contained this small energy interval. Once this average histogram had been completed, a smooth curve was drawn through the midpoints of the tops of the bars. The averaged curve obtained from five histograms ($N=5$) for the self-consistent calculation is indicated by the dashed curve in Fig. 6. It can be seen that the significant difference between this histogram and the averaged curve is the relative heights of the peaks in the d band. However, the agreement is better than can be generally expected and in fact for three out of the other four histograms used to get this averaged curve,

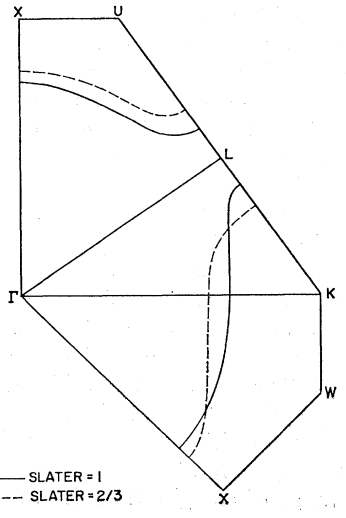

FIG. 5. Intersections of the (100) and (110) planes with the Fermi surface of self-consistent copper.

the peaks varied not only in relative height but were also shifted in energy.

DISCUSSION

The results of the present self-consistent calculations are generally in good agreement with experimental results. As shown in Table III, the width of the d band is somewhat narrower for the calculation in which full exchange was used than it was for either of those previously calculated or for those determined experimentally. However, it can be seen that this narrower width is still in good agreement with Spicer's experimental results. The relative location of the d band with respect to the Fermi energy, namely, $E_f - X_5$, is not in as good agreement with the experimental results as one would like. However, if one considers the value of $E_f - X_5$ for the calculation in which $\frac{2}{3}$ of the exchange was used, the agreement with experiment should be quite good for a calculation involving about 0.8 of the exchange. This is the same factor as that found by Lenander[24] in his calculations on Pr^{3+} and is approximately the same as the $\frac{5}{6}$ found by Herman[25] in his nonrelativistic self-consistent band calculations on germanium.

The width of the d band for such a calculation should also be in good agreement with the experimental results. The effect which the exchange has on the width and location of the d band is shown in Fig. 7. This comparison of density of states curves shows that a self-consistent calculation in which the fraction of the exchange used lies between 1 and $\frac{2}{3}$, should give a density of states curve that would be in excellent agreement with Spicer's experimental curve.[26]

In comparing the neck and belly radii of the Fermi surface, as given in Table IV, the neck radius, resulting from the self-consistent calculation in which the full exchange term was used, is somewhat smaller than that found experimentally by Shoenberg. However, the neck radius, resulting from the calculation in which $\frac{2}{3}$ of the exchange was used, is somewhat larger than the Shoenberg's experimental results. Again, it seems that a fraction of exchange somewhere between 1 and $\frac{2}{3}$ would give results in excellent agreement with experiment. As for the belly radii, those resulting from both calculations for the [100] direction are in reasonably good agreement with the experimental results. However, the belly radii in the [110] direction resulting from both calculations seem somewhat too small. The asphericity of the Fermi surface for both present calculations is somewhat larger than that found by Shoenberg,[27] and the asphericity found by Kamm[28] falls between the two present calculations.

The initial goal was to find which coefficient of the Slater exchange potential gave results in better agreement with experiment. Though the results reported

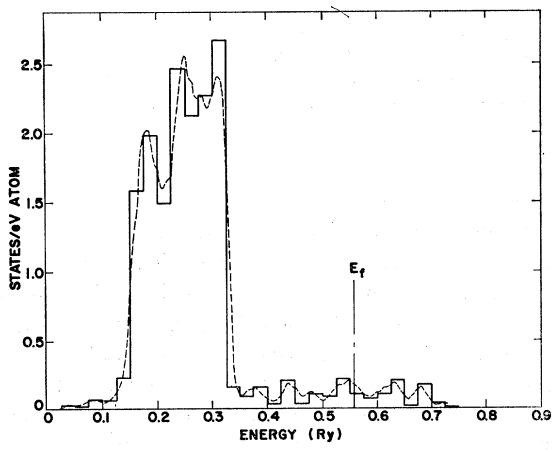

FIG. 6. Density of states histogram and averaged curve for self-consistent copper.

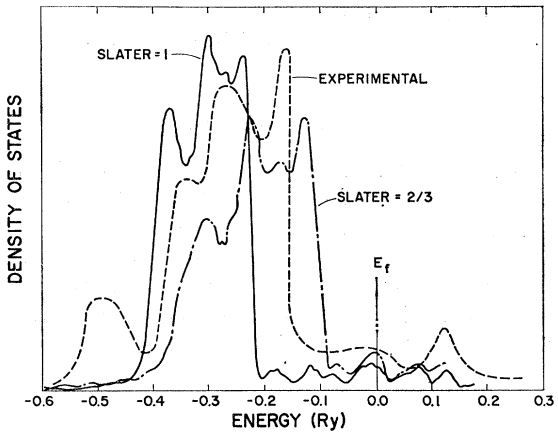

FIG. 7. Comparison of density of states curves from the two present self-consistent calculation with that obtained from photoemission studies by Spicer (Ref. 26).

TABLE IV. Comparison of the present values and those published previously for the neck and belly radii of the Fermi surface for copper (in $Å^{-1}$).

	Neck	Belly
Previous calculations:		
Segall[a]	0.28±0.03	1.33±0.01
Chodorow's[a]	0.20±0.03	1.35±0.02
Experimental:		
Shoenberg[b]	0.28	1.38,1.40
Kamm[c]	...	1.31,1.44
Present calculations:		
Slater = 1	0.22	1.28,1.36
Slater = $\frac{2}{3}$	0.38	1.14,1.44

[a] Reference 16. [b] Reference 27. [c] Reference 28.

[24] C. J. Lenander, Phys. Rev. **130**, 1033 (1963).
[25] F. Herman (private communication).
[26] W. E. Spicer (to be published).
[27] D. Shoenberg, Phil. Mag. **5**, 105 (1960).
[28] G. N. Kamm, Bull. Am. Phys. Soc. **11**, 446 (1966).

here indicate a coefficient between $\frac{2}{3}$ and 1, at the present there is no theoretical justification for such a number.

CONCLUSIONS

From the work reported above, it was concluded that the self-consistent APW method of calculating the energy-band structure of metallic copper yields results that are in reasonably good agreement with experimental results. It was also concluded that the agreement could be improved if a self-consistent APW calculation were carried out in which the exchange was reduced to a fraction somewhere between 1 and $\frac{2}{3}$ of the Slater free-electron approximation.

ACKNOWLEDGMENTS

The authors wish to thank Dr. A. C. Switendick for his considerable help and guidance during all stages of this work. Without his counsel, and without the computer programs which he and Dr. J. H. Wood made available to us, completion of this research would have been considerably delayed. The kind interest and assistance of F. W. Schonfeld and W. N. Miner were also appreciated.

PHYSICAL REVIEW VOLUME 157, NUMBER 3 15 MAY 1967

Effect of Sample Geometry on Magnetomorphic Oscillations in the Hall Effect in Cadmium at Liquid-Helium Temperatures

H. J. MACKEY, J. R. SYBERT, AND J. T. FIELDER
Department of Physics, North Texas State University, Denton, Texas
(Received 19 December 1966)

Size-effect oscillations in the Hall resistivity have been studied in a monocrystal of highly pure cadmium at liquid-helium temperatures. Samples ranging in thickness from 2.01 to 0.09 mm were prepared from a single monocrystal by successively reducing the thickness using spark planing followed by electropolishing. The probes were not removed during this process to ensure that the samples were representative of a common background of orientation, strain, purity, and surface condition. The magnetic field was applied parallel to the hexagonal axis, and dependence on thickness parallel to this direction was studied in the period, phase, and amplitude of the oscillations. The amplitude was observed to increase as thickness was reduced. The oscillations are not strictly periodic, but the apparent period is proportional to the reciprocal thickness. The phase of the oscillations is determined to be zero, although existing theory predicts a phase of $\pi/2$. It is concluded that the lens-shaped pocket of electrons in the third Brillouin zone is responsible for the oscillations. The radius of curvature of the lens apex in the hexagonal direction is determined to be $k_F = 1.37$ Å^{-1}. A study of the temperature dependence of the amplitude of the oscillations implies that the mean free path is in the millimeter range at liquid-helium temperatures. A careful search for short-period oscillations observed by other researchers was fruitless. Data from an electropolished sample were compared to those from a spark-planed sample of the same dimensions; the amplitude of the oscillations was found to be twice as large in the spark-planed sample data as in the electropolished sample data. A slight increase in amplitude was effected by abrading an electropolished sample with No. 600 SiC paper. This enhancement in amplitude implies that an appreciable number of electrons scatter specularly at the electropolished surfaces. It is suggested that a very thin distorted layer at the crystal surface may be necessary to observation of the short-period oscillations.

INTRODUCTION

IN thin metal plates or wires where the mean free path is comparable to or greater than the dimensions of the sample, one must consider the effects of boundary scattering in problems of electron transport. The phenomena introduced by boundary scattering are known as size or morphic effects. The problem of increased resistivity in thin films was first considered as early as 1901 by Thomson.[1] Following that initial attempt, several contributions to the theory have appeared[2–5] and, in recent years, various experiments related to the size-effect phenomena have been reported. Much of this work relates to the case of either longitudinal magnetic fields or zero magnetic field.[6] Sondheimer[7] has treated the case of conductivity in thin samples with a transverse magnetic field. In particular, he predicted oscillations in the Hall effect and transverse magnetoresistance as a function of magnetic field with the magnetic field applied perpendicular to the plane of a thin con-

[1] J. J. Thomson, Proc. Cambridge Phil. Soc. **11**, 20 (1901).
[2] A. C. B. Lovell, Proc. Roy. Soc. (London) **A157**, 311 (1963).
[3] K. Fuchs, Proc. Cambridge Phil. Soc. **34**, 100 (1938).
[4] L. Nordheim, Act. Sci. Ind. No. **131**, (1934).
[5] D. K. C. MacDonald and K. Sarginson, Nature **164**, 921 (1949).
[6] See Ref. 19 for an extensive bibliography.
[7] E. H. Sondheimer, Phys. Rev. **80**, 401 (1950); Advan. Phys. **1**, 1 (1952).